Proceedings of the 9th International Conference on Cyclotrons and their Applications
September 1981, Caen, France

STATUS REPORT ON THE NEUTRON TIME-OF-FLIGHT FACILITY AT THE HAMBURG ISOCHRONOUS CYCLOTRON +)

Y. Holler, R. Langkau, W. Peters, N. Schirm, W. Scobel and R. Wien

Universität Hamburg, I. Institut für Experimentalphysik, Zyklotron, D-2000 Hamburg 50

Abstract.- The present state of the neutron TOF facility at the Hamburg Cyclotron is described and some representative results for fission and preequilibrium neutron spectroscopy are given. The extension of the TOF system being presently under construction is discussed as well as instrumental and detector developments for this facility.

1. Introduction.- The Hamburg Isochronous Cyclotron is an energy variable light ion (p,d,^{3}He,α) accelerator with $E \leq 30$ MeV$\cdot q^2/A$ and operates with RF between 7 and 21 MHz. An external burst suppression system[1] allows to reduce the repetition rate to typically 1 MHz. This way neutron time-of-flight spectroscopy of continuous neutron energy spectra for $E_n \geq 0.6$ MeV can be performed with flight paths of 6-8 m length. So far we have used two organic scintillators NE213 of 2" thickness and 4" or 10" ϕ, respectively. The overall and long term time resolution obtainable is 1.5 ns (2.5 ns) for protons (α particles), where $\geq$ 0.6 ns (1.5 ns) is the contribution of the Cyclotron itself. The whole set up is located on top of the 10×10×4 m neutron hole in the concrete floor; the remaining neutron background is accounted for by supplementing each TOF by a second run with a bar of ∿ 75 cm paraffine being inserted midway between target and detector.

In Sect. 2 we shall give some examples of our recent neutron TOF work; Sect. 3 is devoted to the extension of the TOF capabilities being presently under construction, and Sect. 4 to neutron detector instrumentation development.

2. Results.

2.1 Pre- and postfission neutron emission.- Neutrons emitted in the process of charged particle induced fission of heavy elements may be classified into those emitted from the composite system (prefission, including scission neutrons) and postfission neutrons coming from the accelerated fragments. The emission is in first order isotropic in the respective c.m. system. Therefore separation of these two components can be performed with an iterative procedure from the neutron TOF spectra obtained under the angles $\Theta = 0^o$ and 90^o with respect to the direction of the fission fragments.

We have measured this way the average energies $<\varepsilon(m)>$ and multiplicities $<\nu(m)>$ of the postfission neutrons from the reactions p+^{235,236,238}U for projectile energies between 12.7 and 25.6 MeV; the fragment mass m was obtained[2] from the coincident fission fragment TOF-measurement with typically 3 amu resolution[3]. The average yields $<\nu(m)>$ given in Fig. 1 show the well known sawtooth character which is the more pronounced the higher the target mass is. The structure washes out with increasing excitation energy. From $<\nu(m)>$ and $<\varepsilon(m)>$ the average excitation energy of the fragment:

$$<E^*(m)> = <\nu(m)>(<B_n(m)>+<\varepsilon(m)>) + 0.7<B_n(m)>$$

can be calculated, where $<B_n(m)>$ is the average neutron binding energy; the last term accounts for γ-deexcitation. We find that with increasing excitation energy E^* of the system undergoing fission, a distribution of E^* on the two fragments that is proportional to m, i.e. corresponding to an equilibrated system is approached.

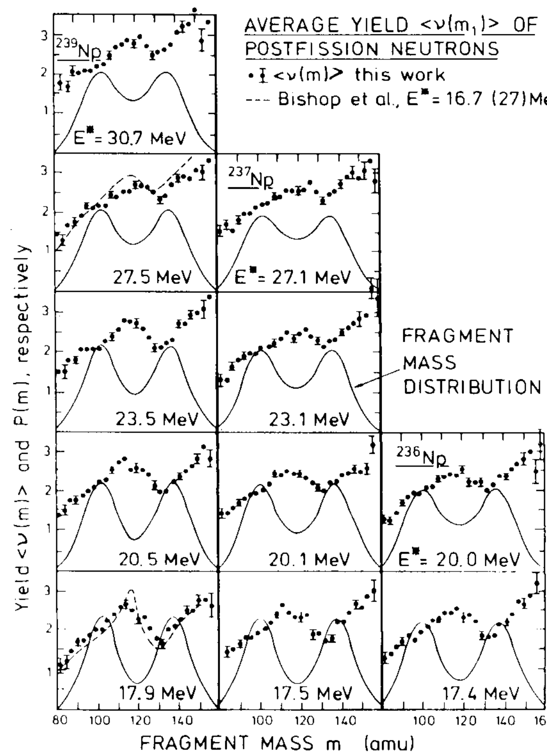

Fig. 1: Yield $<\nu(m)>$ of postfission neutrons per fragment mass m. Solid lines: measured fragment mass distribution P(m) in %.

The average number $<\nu_{is}>$ of prefission neutrons also shows an interesting feature (Fig. 2); it increases with excitation energy E^* (^{236,237,239}Np) in contrast to earlier results[4] and to a full statistical model calculation taking into account the fissility through the double humped barrier (dashed line). We consider this an indication for preequilibrium neutron emission that precedes and suppresses the first chance fission.

2.2 Preequilibrium neutron emission.- The angle integrated energy spectra of protons from (α,xp) reactions for targets in the mass region A≈60 and energies E_α= 23 MeV

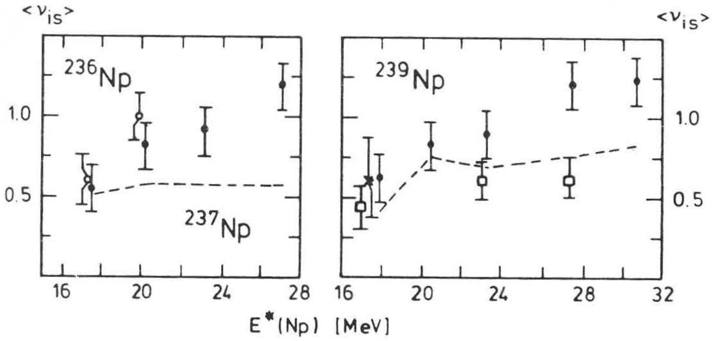

Fig. 2: Average prefission neutron yield for p+U vs. excitation energy E*(Np). Solid and open circles: this work; open squares, Ref. 4.

indicate [5)], that for even-even systems, e.g. $\alpha+^{60}$Ni, the preequilibrium (PE) proton emission corresponds to an initial n_O=4 exciton configuration consisting of 2 neutrons, 2 protons and 0 holes, whereas for odd mass systems like $\alpha+^{59}$Co an n_O=5 (2n, 3p, 0h) configuration seems to be favoured. The interpretation in terms of the unpaired nucleon plus four nucleons from the α particle break up is straight foreward. This odd-even effect should show up in both nucleon exit channels the same way.

We have measured the (α,nucleon) double differential cross sections on ^{59}Co, ^{60}Ni at E_α = 28.5 and 31.5 MeV, respectively. Some representative ^{59}Co(α,xn) data are presented in Fig. 3. They show at high energies and/or foreward angles the features typical for PE emission. In order to deduce the parameter n_O, the angle integrated spectra must be compared with reaction model predictions. A combination of the Ewing-Weißkopf- and the Hybrid PE-model allows a consistent description of both nucleon exit channels with reasonable parameter values, and in particular with n_O=4 (5) for $\alpha+^{60}$Ni ($\alpha+^{59}$Co), if the position of the ground state in the residual nucleus is corrected for pairing with a shift Δ_{uu} = -2.0 MeV, $\Delta_{ug} = \Delta_{gu}$ = -0.7 MeV and Δ_{gg} = 0.6 MeV, respectively.

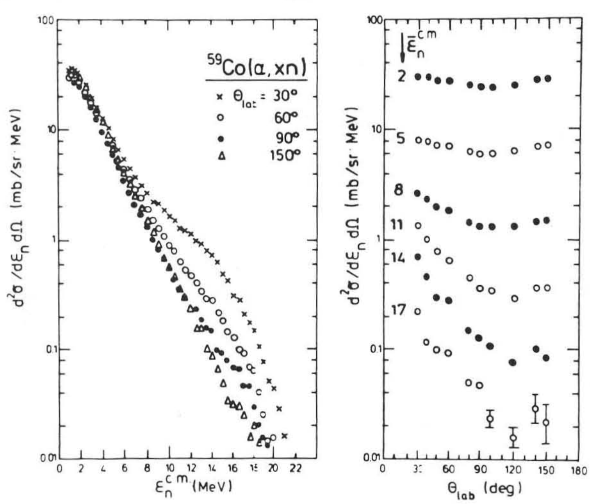

Fig. 3: Energy spectra and angular distributions for 1 MeV bins centered around $\bar{\varepsilon}_n^{\,c.m.}$.

The experiments discussed above have in common that they require TOF spectroscopy of continuous neutron spectra over a broad range of angles. Details of the spectra important for the appraisal of reaction models, e.g. for PE emission, are found in the low intensity region at high energies and backward angles; similarly substantial contributions to the neutron yield may be concentrated to very foreward angles. However, these regions are particularly sensitive to background corrections. We therefore extend our TOF facility to meet the requirements of (1) fixed geometry, (2) low and reproduceable background and (3) access to very foreward and backward angles.

3. Extension of the neutron TOF facility.- The beam delivered to the TOF area is focused by the quadrupole doublet Q1 (ϕ 100 mm) into the neutron fission chamber NF or one of the target positions T1,T2,T3 in the vacuum chamber V. The 2 C-type magnets M1,M2 (gap width 100 mm) between the target positions bend the beam by 17° each. Reaction neutrons from one of the target

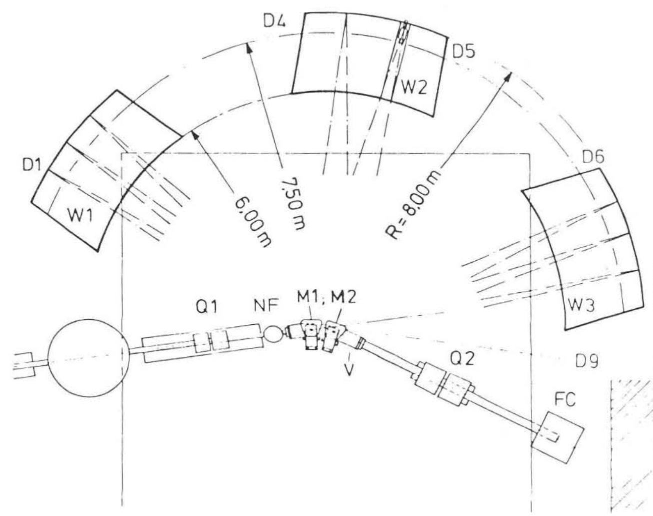

Fig. 4: The new neutron TOF facility at HAIZY. See text for details.

positions enter the flight paths of 7.5 m towards the detectors D1,...,D8 (4"ϕ×2" NE213 on XP2041) through the 2000×91 mm exit window of the chamber V.

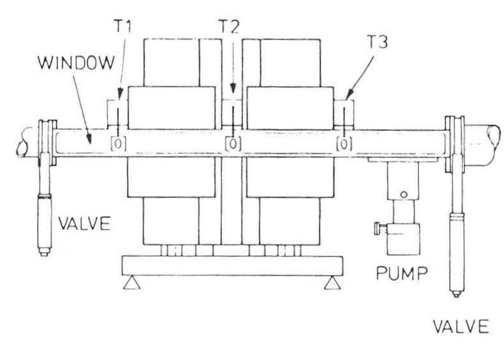

Fig. 5: Side view of magnets M1,M2 and vacuum chamber V.

Combining the 3 target and 8 detector positions we get 24 reaction angles with increments of ≈ 6.5° at small and large and 10.5° at intermediate angles, respectively:

	D1	D2	D3	D4	D5	D6	D7	D8
T1	140.2	133.5	126.8	74.5	63.9	14.9	8.9	3.0
T2	159.2	152.9	146.6	95.4	84.6	33.4	27.1	20.8
T3	177.0	171.1	165.1	116.1	105.5	53.2	46.5	39.8

Tab. 1: Reaction angles accessible.

The additional detector position D9 permits true 0^{o} measurements in connection with target position T2.

The beam tube leading from the target vacuum chamber through the quadrupole doublet Q2 is widened to 200 mm ϕ for guiding the beam, that gets additional divergence due to straggling in the target, without hitting the wall into the segmented, massively shielded faraday cup FC.

Inside the water tanks W1,W2,W3 the detector assemblies are surrounded by 200 mm ϕ collimator tubes. 1.5 m of water and double conical throats made of polyethylene at the entrance shield against stray neutrons coming out of the surroundings of the targets. The alignment of the collimator tubes with respect to the 3 target positions as well as the movement of the targets themselves is done by remote digitally controlled drives.

For a simulation of the neutron background scattered in by the mass of the deflecting magnets, 400 kg of copper were placed in a test measurement directly under and behind the target chamber used up to now. Comparing the data with corresponding ones from open geometry measurements we saw the background in the low energy region roughly doubled. It was accounted for quantitatively by the usual separate background run employing a shadow bar and therefore yielded unchanged net spectra. In summarizing, we have tried to combine in a TOF set up the advantages of a fixed geometry and shielding with the possibility of reaction angle variation by magnetic deflection [6]; it differs from that of [7] by its discrete target positions.

4. Detector instrumentation development.-

When measuring absolute cross-sections for neutron emission an exact knowledge of the detection threshold of the counters in question is essential, especially if one is concerned with continuous spectra containing dominant evaporation components, that are peaking below 1 MeV, i.e. in the detector threshold region. The main sources of uncertainty in the determination of the thresholds are:

(a) the localization of the relative position of the Compton edge within the spectra of γ-calibration sources as measured with the individual detectors,
(b) the energy dependent ratio of the light outputs for Compton electrons and recoil protons,
(c) the gain of the PM-tube varying in time and depending on temperature, current load (counting rate) and its antecedence.

Points (a) and (c) are subject of running or partially finished work.

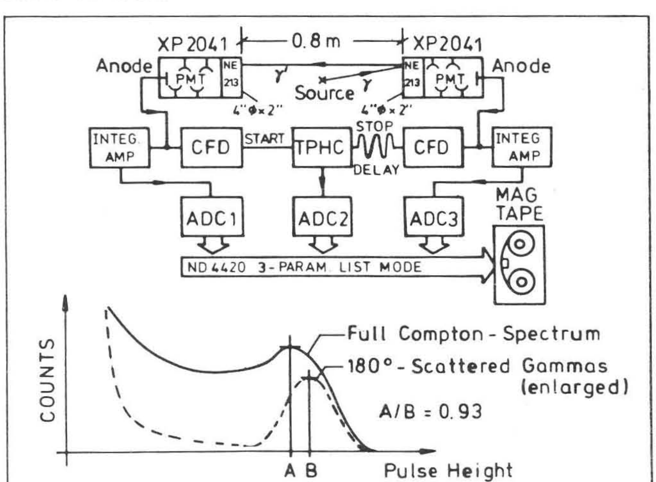

Fig. 6: Set up for Compton edge determination.

ad(a) In a colinear arrangement of 2 counters and a monoenergetic γ-source between them (cf. Fig. 6) one gets by time-of-flight techniques the full Compton spectra as well as the position of the 180^{o} scattered (and detected by the other counter, respectively) γ-quanta for both counters at the same time. The results are to be compared with Monte-Carlo calculations [8] considering also multiple scattering.

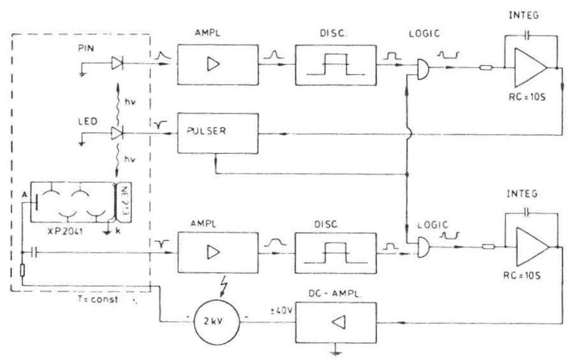

Fig. 7: Detector stabilization: overall instability at $\Delta T \leq 5^{o}K$ for $0 < \nu < 10$ kHz: max. 0.5%.

ad(c) The gain of the PM-tube is inspected and held constant in a regulation loop consisting of a pulsed LED-reference light source, a discriminator and a device for remote control of the high voltage (cf. Fig. 7). The light output of the LED is inspected in a similar loop by a drift free PIN photo diode and forced to its nominal value by regulating the amplitude of the pulse generator driving the LED, Ref. [9]. All of the electronics except the charge sensitive PIN diode preamplifier is contained in a 2/12 NIM case.

References.

1. H. Krause et al., Nucl. Instr. & Meth. 134(1976)15
2. Y. Patin et al., Nucl. Instr. & Meth. 160(1979)471
3. P. Plischke et al., Nukleonika (1981) in press
4. C.J. Bishop et al., Nucl. Phys. A198(1972)161
5. A. Alevra et al., Nucl. Phys. A265(1976)376
6. C.D. Goodman et al., IEEE Trans.Nucl.Sci. NS-26 (1979)2248
7. M.B. Greenfield et al., Phys. Rev. C6(1972)1756
8. G. Dietze, IEEE Trans.Nucl.Sci. NS-26(1979)398
9. W.L. Reiter et al., Nucl. Instr. & Meth. 173(1980) 275

+) Work supported in part by the BMFT.